THE PERTURBATIVE POMERON AND THE CCFM EQUATION *

P.J. SUTTON

Department of Physics and Astronomy
University of Manchester
Brunswick Street, Manchester, M13 9PL
England.

(Received November 15, 1996)

The first part of my talk is a very brief review of the Pomeron and how it is described in perturbative QCD by the BFKL equation. The BFKL Pomeron differs from that observed in total cross sections, but there is some hope that it may be observed in perturbative high energy processes. A particular application of the BFKL equation is to the evolution of the gluon at low x and the consequences that this has on the structure functions, F_2 and F_L. Finally I discuss the CCFM equation which contains both the BFKL and more traditional DGLAP forms of gluon evolution.

PACS numbers: 12.38. Bx

1. Introduction

We currently have an excellent candidate for the theory of the strong interactions, namely Quantum Chromodynamics. However, before the discovery of this theory, physicists instead studied the behaviour of scattering amplitudes at high energies. General properties such as unitarity and analyticity turn out to be strong constraints on the behaviour of such amplitudes, enabling many interesting features to be deduced. This led to the development of a branch of physics known as Regge theory. However, interest in Regge theory declined sharply after the discovery of QCD and asymptotic freedom. Unfortunately even with the full power of perturbation theory at our disposal, predictions for many physical observables remain a highly non-trivial task. Meanwhile the predictions of Regge theory, based as they are on such general properties as analyticity, are still valid. It is

* Presented at the XXXVI Cracow School of Theoretical Physics, Zakopane, Poland, June 1–11, 1996.

an interesting question to see how these predictions compare with those of QCD at high energy. Interest in this problem has been fuelled by the latest generation of colliders which are capable of delivering high centre-of-mass energies. In this contribution I shall only give a brief overview of some of the progress that has been made in this area. Therefore, I recommend that you look in Ref. [1] for more details.

2. Regge Physics and the Pomeron

Regge Physics is concerned with the high energy behaviour of scattering amplitudes expressed in terms of the Mandelstam variables s and t. The properties of analyticity, unitarity and crossing symmetry lead one to the conclusion that the amplitude should behave at high energies as

$$A(s,t) \to s^{\alpha(t)}\,, \tag{1}$$

where the function $\alpha(t)$ is known as the Regge trajectory and is an approximately linear function of t, $\alpha(t) \simeq \alpha_0 + \alpha' t$. For $t > 0$ these trajectories connect particles with similar quantum numbers such that

$$\alpha(m^2) = J\,, \tag{2}$$

where m is the mass and J the spin of the relevant particle. A scattering amplitude which describes an elastic scattering process, $A_{a\to a}(s,t)$, is related via the optical theorem to a total cross section, $\sigma_{\rm tot}(a \to X)$. Regge theory predicts that the high energy behaviour of this total cross section will be

$$\sigma_{\rm tot} \sim s^{\alpha(0)-1}\,. \tag{3}$$

Most Regge trajectories have $\alpha(0) < 1$ and consequently produce contributions to the total cross section which decrease with increasing energy. However, it is observed experimentally that total cross sections do not fall as s increases. Therefore there must be a trajectory with $\alpha(0) \gtrsim 1$. This trajectory is known as the Pomeron trajectory, after Pomeranchuk [2]. A fit by Donnachie and Landshoff [3] to a variety of total cross sections finds

$$\sigma_{\rm tot} \sim s^{0.08}\,. \tag{4}$$

Figure 1 shows their fit to pp and $p\bar{p}$ data. In keeping with the other Regge trajectories we expect that for $t > 0$ that there should be particles lying on this Regge trajectory. Since the Pomeron carries the quantum numbers of the vacuum, these particles correspond to glueballs. The WA91 collaboration at CERN has found just such a candidate glueball state with mass, 1.9 GeV [4].

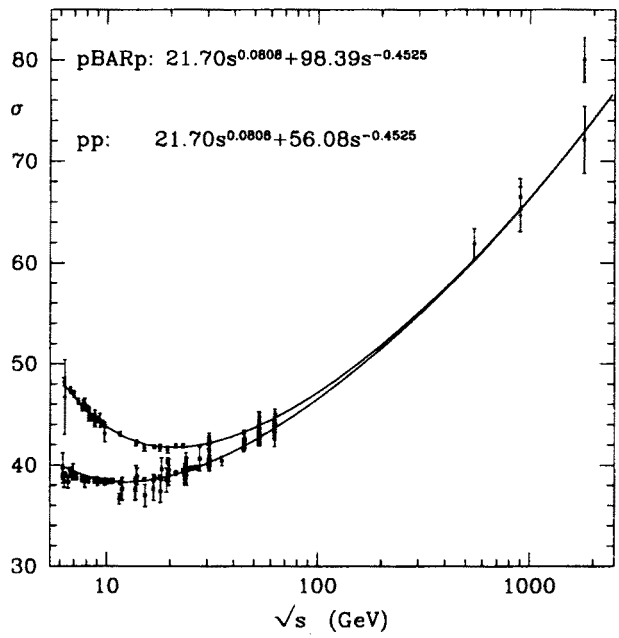

Fig. 1. pp and $p\bar{p}$ total cross sections with the asymptotic behaviour, $s^{0.08}$.

3. The reggeized gluon in QCD

How do the predictions of Regge theory compare with those of QCD? In this section we shall see that the scattering amplitude for colour octet exchange does indeed behave at high energies as $s^{\alpha(t)}$. We consider quark quark scattering with a single gluon exchanged in the t channel. At high energies this behaves as $A_0(s,t) \sim s/t$ which is quite different from the $s^{\alpha(t)}$ behaviour associated with Regge theory. However, we should also consider contributions from higher order graphs which transfer *the quantum numbers* of the gluon. The usual suppression of such contributions due to powers of α_S can be overcome by large logarithms of s. So at the next order in α_S we consider the colour octet contribution from two gluon exchange. We only include the piece which contains the $\ln(s)$ term and, in general, our approach will only include such "leading logarithms". With this in mind it is found that the amplitude at the next order, A_1, is proportional to A_0

$$A_1(s,t) = A_0(s,t)\varepsilon(t)\ln(s)\,. \tag{5}$$

The function $\varepsilon(t)$ (which contains no s dependence) is formally infinite due to an infra-red divergence. However, we can adopt some regularization scheme, such as dimensional regularization, in order to proceed. At the next order things become more complicated due to the greater number of

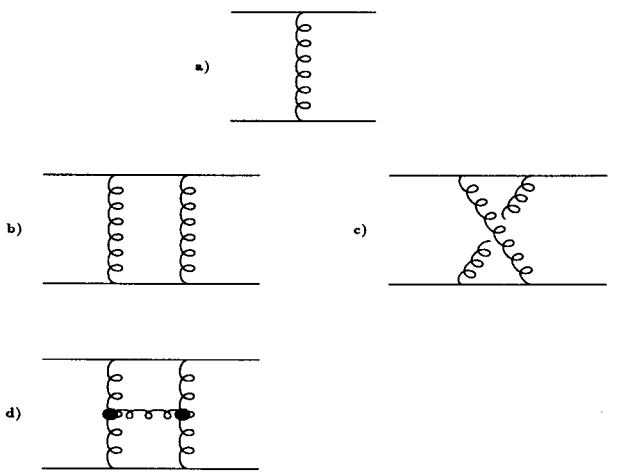

Fig. 2. a) The leading order diagram which gives rise to A_0, b) The first contribution to A_1, c) the crossed contribution to A_1, d) The "one rung" contribution to A_2, built from the effective vertex, Γ.

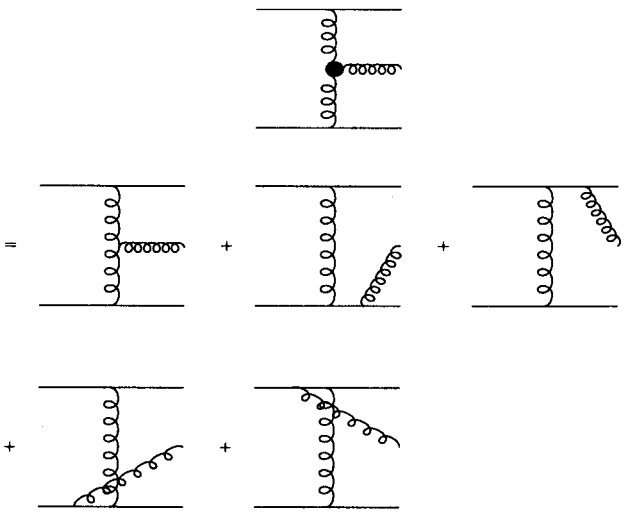

Fig. 3. The effective vertex, Γ represents a combination of various gluon emissions.

possible diagrams. A useful procedure is to introduce an effective vertex, Γ, which summarizes a variety of gluon emission possibilities (Fig. 2 and 3). The contribution from the resulting "one rung" diagram of Fig. 2(d) and

the crossed contribution obtained from $s \leftrightarrow u$ is

$$A_2(s,t) = A_1(s,t)\tfrac{1}{2}\varepsilon^2(t)\ln^2(s) \quad + \quad \text{extra terms}. \tag{6}$$

The extra terms spoil the proportionality of A_2 to A_0. However, they cancel when we include the relevent contributions from three gluon exchange (which is the same order in α_S). We can continue the process to higher orders and we find that each contribution is proportional to the leading contribution A_0

$$A_n(s,t) = A_0(s,t)\varepsilon^n(t)\ln^n(s)/(n!)\,. \tag{7}$$

Our approach is thus leading logarithmic in the sense that we are summing terms $\alpha_S^n \ln^n(s)$ whilst neglecting terms $\alpha_S^n \ln^{n-1}(s)$ and smaller. If we sum up all the leading contributions we obtain

$$\begin{aligned} A(s,t) &= A_0(s,t)\sum_{n=0}^{\infty}\frac{\varepsilon^n(t)\ln^n(s)}{n!} \\ &= A_0(s,t)s^{\varepsilon(t)}\,. \end{aligned} \tag{8}$$

Now recalling that $A_0(s,t) \sim s$ we obtain

$$A(s,t) \sim s^{\alpha(t)}\,, \tag{9}$$

where $\alpha(t) = 1 + \varepsilon(t)$. Thus we see Regge behaviour. We have not cured the problem that $\varepsilon(t)$ is infra-red divergent. However, we shall see that the perturbative Pomeron is free from such divergences.

4. The Pomeron

For the reggeized gluon we considered diagrams which exchanged the quantum numbers of the gluon. The Pomeron, however, corresponds to the quantum numbers of the vacuum. Consequently the simplest model of the Pomeron in QCD is the exchange of two gluons. As in the previous case we also need to sum the leading log s contributions from higher orders. The whole procedure is similar to that of building up the Regge gluon. However, unlike that case, we do not find that the next order amplitude A_1 is proportional to A_0. To circumvent this problem we no longer work in terms of the scattering amplitude. Instead we note that the amplitude for a process involving Pomeron exchange can be written as

$$\frac{\text{Im}\,A(s,t)}{s} = \frac{\mathcal{G}}{(2\pi)^4}\int d^2\boldsymbol{k}_1\, d^2\boldsymbol{k}_2\, \Phi_A(\boldsymbol{k}_1,\boldsymbol{q})\,\frac{F(y,\boldsymbol{k}_1,\boldsymbol{k}_2,\boldsymbol{q})}{\boldsymbol{k}_2{}^2(\boldsymbol{k}_1-\boldsymbol{q})^2}\,\Phi_B(\boldsymbol{k}_2,\boldsymbol{q})\,. \tag{10}$$

Where $\mathcal{G}$ is the colour factor for the process and the two-vectors $\boldsymbol{k}_1$,$\boldsymbol{k}_2$ and $\boldsymbol{q}$ come from a Sudakov decomposition of the corresponding four-vectors ($\boldsymbol{q}$ is simply the momentum transfered in the t channel, so $t = -\boldsymbol{q}^2$). The functions $\Phi_i(\boldsymbol{k}, \boldsymbol{q})$ are called the impact factors and determine the coupling of the Pomeron to the external particles. The function F describes the Pomeron itself and is independent of the external particles. At leading order the function F is just two gluon exchange and so we have

$$F_0 = \delta^2(\boldsymbol{k}_1 - \boldsymbol{k}_2)\,. \tag{11}$$

At the next order in α_S, F_1, contains an extra gluon exchange beween the two t channel gluons (coupled via the effective vertex, Γ) as shown in Fig. 4. This 'one rung' ladder diagram can be expressed in terms of an integral kernel, $\mathcal{K}_{\mathrm{R}}$, acting on the lowest order diagram, F_0

$$F_1 = \mathcal{K}_{\mathrm{R}} \otimes F_0\,. \tag{12}$$

The action of this kernel corresponds to the addition of one "gluon rung"

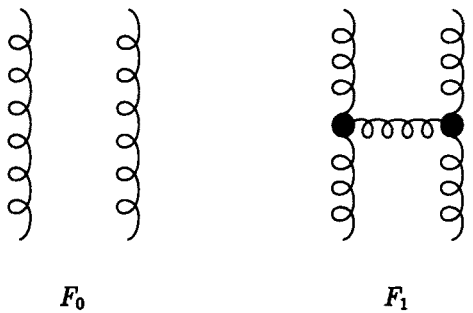

Fig. 4. The Pomeron at lowest order in QCD corresponds to two gluon exchange (colour singlet). The next order consists of the "one rung" diagram with couplings described by the effective vertex, Γ.

to the zero rung diagram. However, it is in fact more general than this. It can be applied to the n^{th} rung diagram to generate the $(n+1)^{\mathrm{th}}$ diagram

$$F_{n+1} = \mathcal{K}_{\mathrm{R}} \otimes F_n\,. \tag{13}$$

The summation of all the leading terms thus leads to an integral equation for F

$$\begin{aligned} F &= F_0 + F_1 + F_2 + \ldots \\ &= F_0 + \mathcal{K}_{\mathrm{R}} \otimes (F_0 + F_1 + \ldots) \\ &= F_0 + \mathcal{K}_{\mathrm{R}} \otimes F\,. \end{aligned} \tag{14}$$

At this stage F contains an infra red divergence. However, we have only considered the real gluon emission terms. We have as yet to take into account the necessary virtual corrections, $\mathcal{K}_V$. This is achieved by replacing the normal t channel gluons by reggeized gluons. As a result the kernel is modified to $\mathcal{K} = \mathcal{K}_R + \mathcal{K}_V$. Now the infra-red divergences cancel between the real and virtual pieces and the resulting F is a finite quantity. So in summary, the *perturbative* QCD Pomeron consists of a ladder built

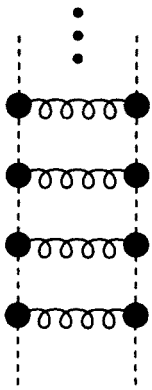

F

Fig. 5. The BFKL Pomeron consists of a ladder built from reggeized gluons.

from reggeized gluons in the t channel connected together by normal gluon "rungs" at effective vertices, Γ. The integral kernel which generates this Pomeron was first calculated by Balitsky, Fadin, Kuraev and Lipatov and leads to the famous BFKL equation [5].

5. The BFKL equation

The BFKL equation can be solved by finding the eigenfunctions of the kernel $\mathcal{K}$. Although these have been found for the general case [6] of finite momentum transfer ($|t| > 0$) we shall look at the particular case $|t| = 0$. This is much simpler yet it is still extremely useful. For example, it yields the value of the Pomeron intercept, $\alpha_{\mathrm{BFKL}}(0)$. To simplify the y dependence of the BFKL equation, we consider the Mellin transfer of F

$$f(\omega, \boldsymbol{k}_1, \boldsymbol{k}_2, 0) = \int dy\, e^{-\omega y}\, F(y, \boldsymbol{k}_1, \boldsymbol{k}_2, 0)\,. \tag{15}$$

So the BFKL equation takes the form

$$\omega f(\omega, \boldsymbol{k}_1, \boldsymbol{k}_2, 0) = \delta^2(\boldsymbol{k}_1 - \boldsymbol{k}_2) + \mathcal{K} \otimes f(\omega, \boldsymbol{k}_1, \boldsymbol{k}_2, 0)\,. \tag{16}$$

The integral kernel in this case takes the form

$$\mathcal{K} \otimes f(\omega, \boldsymbol{k}_1, \boldsymbol{k}_2, 0) = \frac{\overline{\alpha}_S}{\pi} \int d^2\boldsymbol{k}' \frac{1}{(\boldsymbol{k}_1 - \boldsymbol{k}')^2}$$
$$\times \left(f(\omega, \boldsymbol{k}', \boldsymbol{k}_2, 0) - \frac{{\boldsymbol{k}_1}^2}{({\boldsymbol{k}'}^2 + (\boldsymbol{k}_1 - \boldsymbol{k}')^2)} f(\omega, \boldsymbol{k}_1, \boldsymbol{k}_2, 0) \right) . \qquad (17)$$

Here $\overline{\alpha}_S = 3\alpha_S/\pi$. We expand f in terms of the complete set of eigenfunctions, ψ_ν of the integral kernel, $\mathcal{K}$ with eigenvalues, $\lambda(\nu)$

$$f(\omega, \boldsymbol{k}_1, \boldsymbol{k}_2, 0) = \int d\nu \; a_\nu(\boldsymbol{k}_1) \psi_\nu(\boldsymbol{k}_2) . \qquad (18)$$

Substituting this into the BFKL equation (16) we obtain

$$\int d\nu \; (\omega - \lambda(\nu)) \; a_\nu(\boldsymbol{k}_2) \; \psi_\nu(\boldsymbol{k}_1) = \delta^2(\boldsymbol{k}_1 - \boldsymbol{k}_2) . \qquad (19)$$

Using the orthogonality of the eigenfunctions

$$\int d\nu \; \psi^*_\nu(\boldsymbol{k}_2) \; \psi_\nu(\boldsymbol{k}_1) = \delta^2(\boldsymbol{k}_1 - \boldsymbol{k}_2) \qquad (20)$$

we find that the solution of the BFKL equation is given by

$$f(\omega, \boldsymbol{k}_1, \boldsymbol{k}_2, 0) = \int d\nu \; \frac{1}{(\omega - \lambda(\nu))} \; \psi^*_\nu(\boldsymbol{k}_2) \psi_\nu(\boldsymbol{k}_1) . \qquad (21)$$

The eigenfunctions are found to be of the form

$$\psi^n_\nu(k) = \frac{1}{\pi\sqrt{2}} (k^2)^{-1/2+i\nu} \; e^{in\phi} , \qquad (22)$$

where ν is a real number $(-\infty < \nu < \infty)$. and ϕ is the angle of $\boldsymbol{k}$ in radial co-ordinates. At high energies, only the $n = 0$ set of eigenfunctions are relevent. For these eigenfunctions the corresponding eigenvalues are found to be $\overline{\alpha}_S \chi(\nu)$, where the function $\chi(\nu)$ is given by

$$\chi(\nu) = 2\psi(1) - \psi(1/2 + i\nu) - \psi(1/2 - i\nu) . \qquad (23)$$

Here $\psi(z)$ is the logarithmic derivative of the gamma function, $\Gamma(z)$. So the solution of the BFKL equation can be written as

$$f(\omega, k_1^2, k_2^2, 0) = \frac{1}{2\pi^2} \int_{-\infty}^{+\infty} d\nu \; \frac{1}{\omega - \overline{\alpha}_S \chi(\nu)} \; (k_1^2)^{-1/2+i\nu} (k_2^2)^{-1/2-i\nu} . \qquad (24)$$

Notice that since ν is a continuous variable we find a cut rather than an isolated pole in the ω plane. Inverting the Mellin transform via

$$F(y, k_1^2, k_2^2, 0) = \frac{1}{2\pi i} \int_C d\omega \; e^{+\omega y} \; f(\omega, k_1^2, k_2^2, 0) \tag{25}$$

leads to

$$F(y, k_1^2, k_2^2, 0) = \frac{1}{2\pi^2} \int d\nu \; e^{\overline{\alpha}_S \chi(\nu) y} \; (k_1^2)^{-1/2+i\nu} (k_2^2)^{-1/2-i\nu} \, . \tag{26}$$

This is an exact solution, but we can perform the ν integration if we make an approximation. We notice that the solution is dominated by small values of ν and so we expand $\chi(\nu)$ about $\nu = 0$

$$\chi(\nu) = 4 \ln 2 - 14\zeta(3)\nu^2 + \ldots \tag{27}$$

Here $\zeta(z)$ is the Riemann zeta function. Keeping only the first two terms in the expansion of $\chi(\nu)$ allows the integral to be performed and F is thus found to behave as

$$F(y, k_1^2, k_2^2, 0) \simeq \frac{1}{\sqrt{k_1^2 k_2^2}} \frac{e^{\omega_0 y}}{\sqrt{4\pi^2 a^2 y}} \exp\left(\frac{-\ln^2(k_1^2/k_2^2)}{4a^2 y} \right) , \tag{28}$$

where $\omega_0 = 4 \ln 2 \overline{\alpha}_S$ and $a^2 = 14 \overline{\alpha}_S \zeta(3)$. Now since $y = \ln(s)$ we see from (10) that the high energy behaviour of a scattering amplitude with $|t| = 0$ Pomeron exchange is

$$A(s,t) \sim \frac{s^{1+\omega_0}}{\sqrt{\ln s}} \, . \tag{29}$$

The Regge intercept is $\alpha_{\mathrm{BFKL}}(0) = 1 + 4 \ln 2 \overline{\alpha}_S \simeq 1.5$ which should be compared with the Donnachie, Landshoff value [3] of $\alpha_{\mathrm{DL}} = 1.08$. The perturbative Pomeron is thus very different from the Pomeron of hadronic physics, however, although it is not visible in total cross section data it may show up in other physical processes.

6. Phenomenology of the BFKL Pomeron

The most immediate application of the BFKL equation is to the evolution of the gluon distribution at low x [1]. To achieve this we connect a suitable (non-perturbative) gluon–hadron impact factor to the lower end of

[1] The reason that the BFKL equation is relevant to low x is because Bjorken x is defined via $x = Q^2/s$, and so high energy corresponds to low x.

our BFKL ladder. We then note that the n rung ladder is related via the optical theorem to the n gluon emission part of the gluon evolution. We have

$$f_g(x,k^2) = f_g^0(x,k^2) + \frac{\overline{\alpha}_S}{2\pi}\int_x^1 \frac{dx'}{x'}\int dk'^2\, \mathcal{K}(k,k')f_g(x',k'^2)\,. \tag{30}$$

Here, the BFKL kernel takes the form

$$\int dk'^2\, \mathcal{K}(k,k')f_g(x',k'^2) = \overline{\alpha}_S\, k^2 \int_0^\infty \frac{dk'^2}{k'^2} \times \left\{ \frac{f_g(x',k'^2) - f_g(x',k^2)}{|k^2-k'^2|} + \frac{f_g(x',k^2)}{(4k'^4+k^4)^{1/2}} \right\}, \tag{31}$$

and where $f_g^0(x,k^2)$ is the "zero rung" term. The gluon distribution is given by integrating over the possible transverse momenta, up to some maximum value determined by an external scale

$$xg(x,Q^2) = \int_0^{Q^2} \frac{dk^2}{k^2}\, f_g(x,k^2)\,. \tag{32}$$

The inhomogeneous term, $f_g^0(x,k^2)$ is expected to have only a weak dependence on x (at least at small x) and so the BFKL equation predicts that

$$f_g(x,k^2) \simeq \frac{x^{-\lambda}}{\sqrt{\ln(1/x)}}\,, \tag{33}$$

where $\lambda = 4\ln 2\overline{\alpha}_S$. So the BFKL equation predicts a steep growth in the gluon distribution as $x \to 0$. This has implications for the structure functions, $F_2(x,Q^2)$ and $F_L(x,Q^2)$. The k_T–factorization prescription [7] allows us to determine F_2 from f_g and a coefficient function, F_0 which describes (off-shell) photon–gluon fusion, $\gamma^* g^* \to q\bar{q}$. Using k_t–factorization, we find

$$F_2(x,Q^2) = \int_x^1 \frac{dx'}{x'} \int \frac{dk^2}{k^2}\, F_0(x/x',k^2,Q^2)\, f_g(x',k^2)\,. \tag{34}$$

The $x^{-\lambda}$ behaviour of f_g filters through into F_2 so that BFKL predicts that at small x

$$F_2(x,Q^2) \sim x^{-\lambda}\,. \tag{35}$$

So that the structure function, F_2 will also rise rapidly in the small x region. Of course this last statement is only true asymptotically. For comparison with actual data, for example from the HERA collider, it is necessary to use (34) and to include some (essentially x independent) background [8].

There is, however, a serious problem associated with the BFKL equation at $t = 0$. The solution behaves as

$$\frac{f(x,k^2)}{(k^2)^{1/2}} \simeq \frac{x^{-\lambda}}{\sqrt{\ln(1/x)}} \exp\left(-\frac{\ln^2(k^2/k_0^2)}{\ln(1/x)}\right). \tag{36}$$

This is a Gaussian-like distribution which is peaked at $k^2 = k_0^2$ and with a width which increases as x decreases. The physical interpretation of this formula is that the typical gluon momenta in the BFKL ladder, described by, k^2, diffuse around a central value, k_0^2 which is determined by the lower impact factor. For a hadron this lower scale is $k_0^2 \simeq 1$ GeV^2 and so the gluon momenta can diffuse into the non-perturbative region where the BFKL equation is no longer valid. One way of avoiding this problem is to couple the BFKL ladder to an impact factor which has a much higher, k_0^2. Such an impact factor could be provided by a parton with a large transverse momentum, $k_T^2 \simeq Q^2$, which would show up in the final state as an extra jet. This process has been studied both theoretically [9] and experimentally [10] and the inital results look encouraging. Finally we mention that some recent progress has been made in understanding the phenomenology of the BFKL equation for $|t| > 0$ and how it relates to the diffractive production of vector mesons [11].

7. The CCFM equation

Finally we return to the problem of gluon evolution at low x. There exists a theoretical framework which gives a unified treatment of both the BFKL ($\ln(1/x)$) evolution and the more familiar DGLAP ($\ln(Q^2)$) evolution. This has been provided by Catani, Ciafaloni, Fiorani and Marchesini (CCFM)[12]. It is based on the coherent radiation of gluons, which leads to an angular ordering of the gluons along a chain of multiple emissions.

Like the BFKL equation, the CCFM equation is defined in terms of an *unintegrated* gluon density, F, which specifies the chance of finding a gluon with longitudinal momentum fraction x and transverse momentum of magnitude k_T. However, this distribution now also depends on some external scale, Q,

$$F(x,k_T^2,Q^2) = F^0(x,k_T^2,Q^2) + \int_x^1 dz \int \frac{d^2q}{\pi q^2}\Theta(Q-zq)\Delta_S(Q,zq)\tilde{P}(z,q,k_T)F\left(\frac{x}{z},k_T'^2,q^2\right). \tag{37}$$

The inhomogeneous or "no-rung" contribution, F^0, may again be regarded as the non-perturbative term coming from the lower impact factor. The function $\tilde{P}$ is the gluon–gluon splitting function

$$\tilde{P} = \overline{\alpha}_S \left[\frac{1}{1-z} + \Delta_R \frac{1}{z} - 2 + z(1-z) \right], \tag{38}$$

where $\overline{\alpha}_S \equiv 3\alpha_S/\pi$. The multiplicative factors Δ_S and Δ_R cancel the singularities manifest as $z \to 1$ and $z \to 0$ respectively. The Sudakov form factor is given by

$$\Delta_S(q, z'q') = \exp\left(- \int_{(z'q')^2}^{q^2} \frac{dk^2}{k^2} \int_0^1 dx \frac{\overline{\alpha}_S}{1-z} \right). \tag{39}$$

It contains the virtual corrections which give rise to the usual 'plus prescription' present in the gluon splitting function. The Regge form factor is given by

$$\Delta_R(z, q, Q_T) = \exp\left(-\overline{\alpha}_S \int_z^{z_0} \frac{dz'}{z'} \int \frac{dk^2}{k^2} \Theta(Q_T^2 - k^2) \Theta(k - z'q) \right) \tag{40}$$

$$= \exp\left(-\overline{\alpha}_S \log\left(\frac{z_0}{z}\right) \log\left(\frac{Q_T^2}{z_0 z q^2}\right) \right), \tag{41}$$

where

$$z_0 = \begin{cases} 1 & \text{if} \quad (Q_T/q) \geq 1 \\ Q_T/q & \text{if} \quad z < (Q_T/q) < 1 \\ z & \text{if} \quad (Q_T/q) \leq z\,. \end{cases}$$

Unlike Δ_S, the Regge form factor Δ_R is not just a function of the branching variables, but depends on the history of the cascade via

$$Q_T = |\boldsymbol{q}_T + \boldsymbol{q}'_T + \boldsymbol{q}''_T + \ldots|. \tag{42}$$

At large x we can set $\Delta\Delta = 1$ and unfold Δ_S to obtain the usual DGLAP equation for gluon evolution. At small x we keep only the $1/z$ piece of P_{gg} and set $\Delta_S = 1$ and unfold $\Delta\Delta$ to obtain the BFKL evolution.

8. Numerical solution of the CCFM equation

We have studied the CCFM equation at small x. In this region we may simplify the equation (37) as follows [13]

$$F(x,k_T^2,Q^2) = F^0(x,k_T^2,Q^2) + \overline{\alpha}_S \int_x^1 \frac{dz}{z} \int \frac{d^2q}{\pi q^2} \times \Theta(Q - zq)\Delta_{\mathrm{R}}(z,q,k_T) F\left(\frac{x}{z}, (\boldsymbol{k}_T + \boldsymbol{q})^2, q^2\right). \quad (43)$$

We take the scale of the running coupling, α_s, to be k_T^2 and we choose F^0 such that it would generate a "flat" gluon, $xg \sim 3(1-x)^5$, in the absence of angular ordering and the $\Delta\Delta$ correction term [13]. With these choices we solve (43) by iteration from the starting distribution. Fig. 6 shows our solution in terms of the integrated gluon distribution, $xg(x,Q^2)$. Also shown are the corresponding solutions for the BFKL equation and the double-leading-logarithm (DLL) approximation to the DGLAP equations.

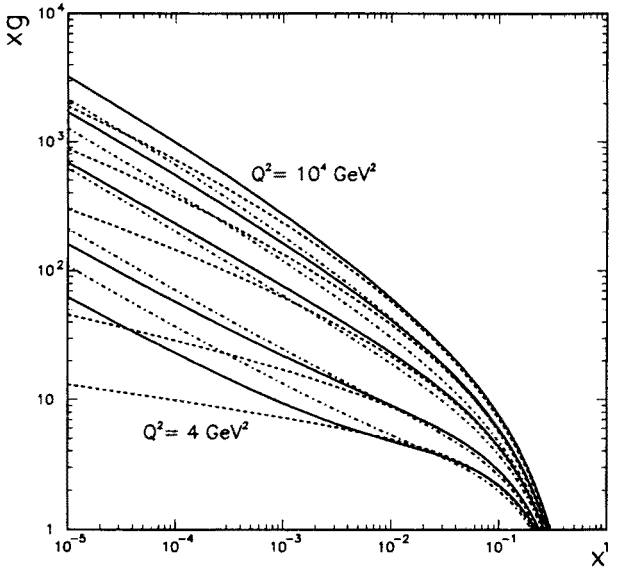

Fig. 6. The integrated gluon distribution xg versus x, obtained from the CCFM (continuous curves), BFKL (dot-dash curves) and the DLL (dashed curves) integral equations, for $Q^2 = 4, 10, 10^2, 10^3$ and 10^4 GeV^2. Our solutions are obtained from a "flat" gluon input [13]

To quantify the increase in xg, we show in Fig. 7 the effective value of λ, defined by

$$xg(x,Q^2) = Ax^{-\lambda}. \quad (44)$$

For small x we see that the solutions converge to a typical $x^{-0.5}$ behaviour, approximately independent of Q^2, which is consistent with that obtained from the solution of the BFKL equation, although the onset of the $x^{-\lambda}$ form is more delayed for the CCFM solution.

The gluon distribution itself is, of course, not an observable. However, as we have seen, the behaviour of the gluon feeds through into physical quantities such as the structure functions. We have therefore calculated the structure function F_2 from the unintegrated gluon distribution F using the usual k_T-factorization procedure. Details of this calculation can be found in Ref. [14].

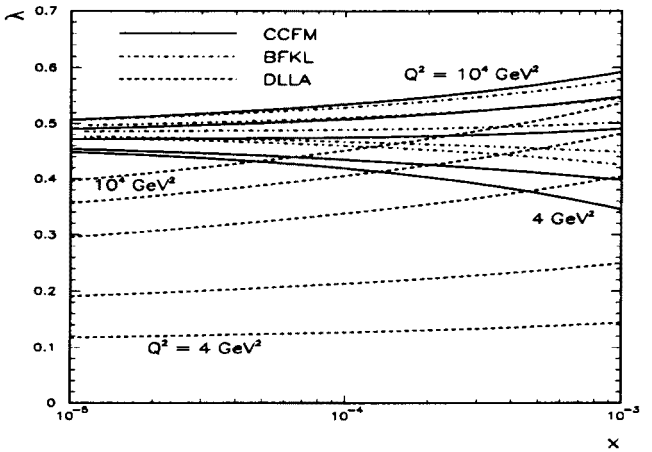

Fig. 7. The effective values of λ, defined by $xg = Ax^{-\lambda}$. The CCFM values (continuous curves) are compared with those obtained from the BFKL (dot-dashed curves) and DLL approximations (dashed curves). In each case we show curves corresponding to five different values of Q^2.

9. Summary

We have seen that the perturbative Pomeron described by the BFKL equation is very different from the Pomeron observed in hadronic total cross sections. The later has an intercept of $\alpha_{\rm DL}(0) \simeq 1.08$ whilst the BFKL equation predicts $\alpha_{\rm BFKL}(0) \simeq 1.5$. However, the BFKL pomeron may be visible in high energy perturbative processes such as the diffractive production of vector mesons. Due to the optical theorem it also has consequences for the gluon distribution at low x and consequently the structure functions, F_2 and F_L. Although the resulting BFKL description of gluon evolution is quite different from the traditonal DGLAP approach, there exists a unified equation (CCFM) which contains both. We have studied this equation and observed a transition from DGLAP-like behaviour at large x to the $x^{-0.5}$ growth predicted by the BFKL equation.

I would like to thank the organisers for their hospitality, in particular Marek Jezabek. Thanks also to Dr. J. Forshaw, Professor A.D. Martin and Professor J. Kwieciński.

REFERENCES

[1] J.R. Forshaw, D.A. Ross, *Quantum Chromodynamics and the Pomeron*, Cambridge University Press, 1997.

[2] I.Y. Pomeranchuk, *Sov. Phys.* **3**, 306 (1956).

[3] A. Donnachie, P. Landshoff, *Phys. Lett.* **B296**, 227 (1992).

[4] S. Abatzis *et al.*, *Phys. Lett.* **B324**, 509 (1994).

[5] E.A. Kuraev, L.N. Lipatov, V. Fadin, *Zh. Eksp. Teor. Fiz.* **72**, 373 (1977) [*Sov. Phys. JETP* **45**, 199 (1977)]; Ya.Ya. Balitskij, L.N. Lipatov, *Yad. Fiz.* **28**, 1597 (1978) [*Sov. J. Nucl. Phys.* **28** 822 (1978)]; L.N. Lipatov, in *Perturbative QCD*, ed. A.H. Mueller, World Scientific, Singapore 1989, p.411; J.B. Bronzan, R.L. Sugar, *Phys. Rev.* **D17** 585 (1978).

[6] L. Lipatov, *Sov. Phys. JETP* **63**, 904 (1986).

[7] S. Catani, M. Ciafaloni, F. Hautmann, *Phys. Lett.* **B242**, 97 (1990); *Nucl. Phys.* **B366**, 657 (1991); J.C. Collins , R.K. Ellis, *Nucl. Phys.* **B360**, 3 (1991); E.M. Levin, M.G. Ryskin, A.G. Shuvaev, *Sov. J. Nucl. Phys.* **53**, 657 (1991).

[8] A.J. Askew, J.Kwieciński, A.D. Martin, P.J. Sutton, *Phys. Rev.* **D49**, 4402 (1994); A.J. Askew *et al.*, *Phys. Lett.* **B325**, 212 (1994).

[9] A.H. Mueller, *Nucl. Phys. B Proc. Suppl.* **18C**, 125 (1990) and *J. Phys.* **G17**, 1443 (1991); J. Bartels, A. De Roeck, M. Loewe, *Z. Phys.* **C54**, 635 (1992); *Nucl. Phys. B Proc. Suppl.* **29A**, 61 (1992); J. Kwiecinski, A.D. Martin, P.J. Sutton, *Phys. Rev.* **D46**, 921 (1992); J. Kwiecinski, A.D. Martin, P.J. Sutton, *Phys. Lett.* **B287**, 254 (1992).

[10] H1 collaboration: S. Aid *et al.*, *Phys. Lett.* **B356**, 118 (1995); J. Bartels *et al.*, DESY preprint 96-036.

[11] J.R. Forshaw, M.G. Ryskin, *Z. Phys.* **C68**, 137 (1995).

[12] M. Ciafaloni, *Nucl. Phys.* **B296**, 49 (1988); S. Catani, F. Fiorani, G. Marchesini, *Phys. Lett.* **B234**, 339 (1990); *Nucl. Phys.* **B336**, 18 (1990); G. Marchesini, in Proceedings of the Workshop "QCD at 200 TeV", Erice, Italy 1990, edited by L. Cifarelli, Yu.L. Dokshitzer, Plenum Press, New York 1992, p.183; G. Marchesini, *Nucl. Phys.* **B445**, 49 (1995).

[13] J. Kwieciński, A. D. Martin, P. J. Sutton, *Phys. Rev.* **D52**, 1445 (1995).

[14] J. Kwieciński, A.D. Martin, P.J. Sutton, *Phys. Rev.* **D53**, 6094 (1996); A.D. Martin, J. Kwieciński, P.J. Sutton, *Z. Phys.* **C71**, 585 (1996).